

SYNTHESIS AND CHARACTERIZATION OF PbS NANOSTRUCTURES TO COMPARE WITH BULK

A. K. MISHRA*, S. SAHA

Department of Physics, Vidyasagar University, Midnapore, Pin 721102, West Bengal, India

Simple chemical reduction route is taken for growth of PbS nanostructure by using ethylene-diamine (EDA) as capping agent. Anhydrous lead chloride, sulphur, NaBH₄ is taken as reactants. Different types of nanostructures are obtained by varying growth time and temperature. The room temperature synthesis of PbS nanoparticles in EDA medium produces high quality nanocrystals as shown by electron microscopy, optical and fluorescence measurements. It is observed that nanoparticles are larger in size for longer growth time as well as higher temperature. Structural and optical properties show that quantum confinement of PbS nanoparticles is good in EDA medium.

(Received December 28, 2019; Accepted March 16, 2020)

Keywords: PbS nanoparticles, Structural properties, Optical properties, Fluorescence life time

1. Introduction

Recently researchers show interest in lead sulfide (PbS) nanoparticles due to its different structural, optical, photo conducting properties which cannot be availed from their bulk materials [1-4]. PbS nanoparticles are much applicable in solar cell, photo detector, laser, LED etc for large Bohr exciton radius (20 nm), shape as well as size tunable properties. Interestingly, group II-VI semiconductor nano particles are extensively used in nano devices [5-7]. The multiple exciton generation process in PbS is immensely helpful to increase efficiency in photovoltaic devices [8]. PbS has huge potential in the field of electrochemical biosensors. Our focus is on emerging application of PbS nanoparticle in efficient antimicrobial agent [9]. When the size of nanoparticles (NPs) decreases band gap increases from direct bulk band gap 0.42 eV at 300K due to quantum confinement effect. Also PbS nano has thousand time greater optical response of same size CdS nano. A number of methods can be followed to grow PbS nanostructure [10-15]. Some of the methods cause environmental hazards and required high temperature [16-20]. Aliphatic ligands have stabilizing and passivating property [21-22]. It bounds PbS quantum dot (QD) in colloidal solutions and control their dimension [23-26]. The produced NPs are highly crystalline and have better solution process ability.

In this work a simple reduction method utilize which is hazard free and does not require high temperature. This work will symbolize a big step forward on the journey to low-cost and high-reproducibility of PbS NPs for photo voltaic devices.

2. Experimental

PbS nanoparticles were prepared with lead chloride, sulfur powder and varying the chemical reagent sodium borohydride in three different molar ratios as 1:1:1, 1:1:3 and 1:1:5. In case of 1:1:1 ratio, firstly at room temperature (25°C), 60 ml ethylene-diamine was taken in a beaker and 2.78 gm PbCl₂, 0.32 gm S and 0.37 gm NaBH₄ were added and kept under stirring for 4 hrs. Then the solution was centrifuged and put on filter paper in funnel for filtration in a nice

* Corresponding author: anjanmishra2011@gmail.com

clean and dust free space. PbS nano powder was collected after drying. This same procedure was followed for another ratio 1:1:3 and 1:1:5. Also for other temperature and time the same process were repeated in EDA medium. We varied time duration of growth (8hrs,12hrs) and different temperatures (10°C,40°C) for ratios 1:1:1 and 1:1:3.

For bulk PbS growth, lead (II) acetate, 3 hydrate and thiourea were used. The reaction was done with 0.66 gm of $(\text{CH}_3\text{COO})_2\text{Pb}\cdot 3\text{H}_2\text{O}$ and 0.17 gm of $\text{CH}_4\text{N}_2\text{S}$ and also base medium having pH level (10-12) was maintained by introducing ammonium hydroxide. No capping material was used during the synthesis of bulk PbS.

High resolution Rigaku Mini Flex X-ray Diffractometer was used to get X-ray diffraction (XRD) pattern of PbS nano powder. Transmission electron microscopy (TEM) images were captured by JEOL-JEM-2100 for various samples. JEOL-JSM 5800 was used to obtain scanning electron microscopy (SEM) image of powder samples. EDX analysis was recorded also. Optical absorption spectra were acquired by using Agilent Technologies Cary 5000 Series UV-VIS-NIR Spectrophotometer. Fluorescence life time measurement was carried out by using step one Plus 96WELL RTPCR system.

3. Results and discussion

3.1. XRD characterization

XRD pattern for PbS nanostructure for particular growth time and temperature are shown in Fig. 1, 2 and 3.

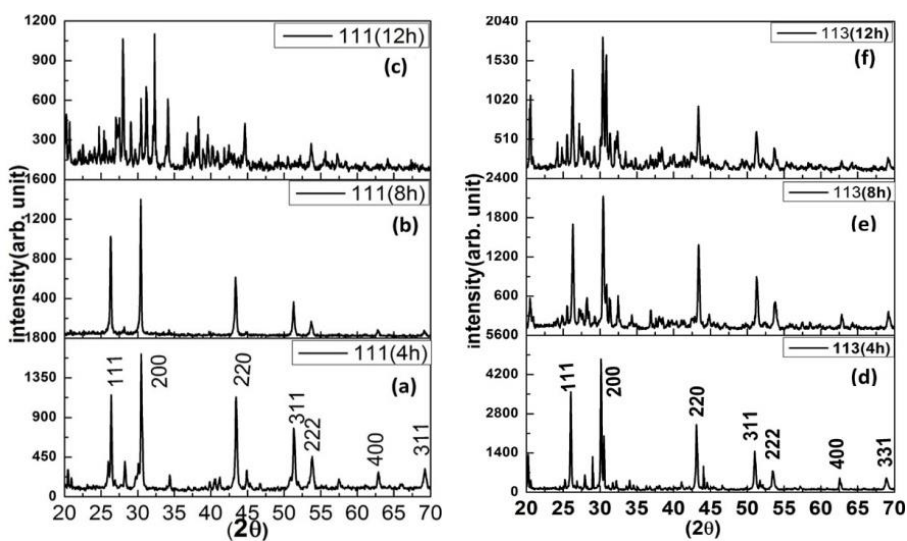


Fig. 1. XRD pattern of PbS (1:1:1) sample in different growth time (a) 4h, (b) 8h, (c) 12h and of PbS (1:1:3) sample in different growth time (d) 4h, (e) 8h, (f) 12h.

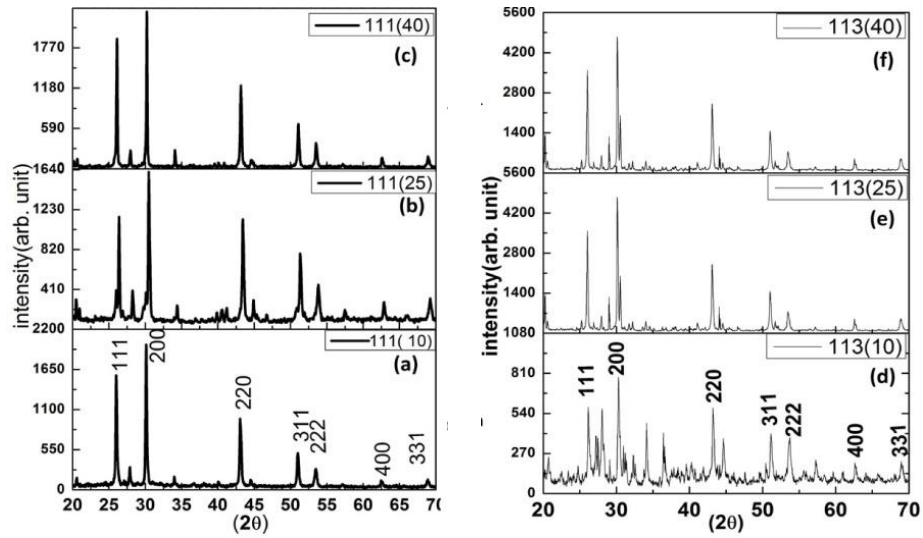


Fig. 2. XRD pattern of PbS(1:1:1) sample in different growth temperatures (a) 10 °C, (b) 25°C,(c) 40 °C and PbS (1:1:3) sample in growth temperatures (d) 10 °C, (e) 25 °C,(f) 40 °C.

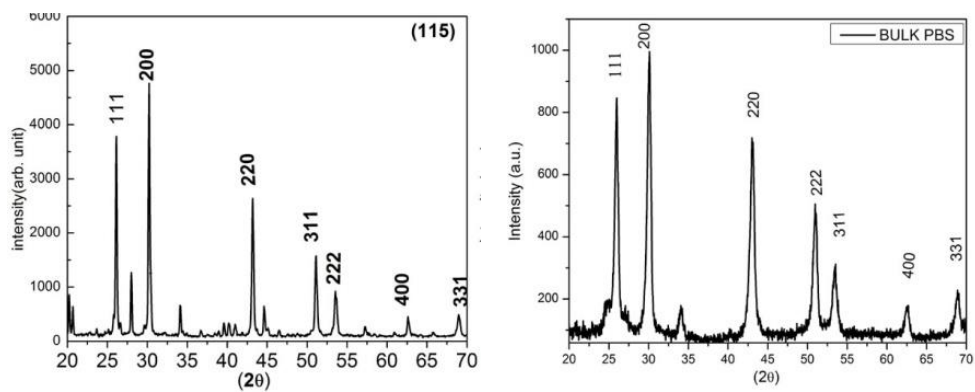


Fig. 3. XRD images of PbS grown at 1:1:5 ratio and Bulk PbS.

XRD patterns of PbS nano particles show well distinct but broad diffraction peaks signifying the formation of nanocrystalline materials. It proves that in case of PbS all the major crystalline planes are present. Bragg's law $2d \sin\theta = \lambda$ is used to find interplanar spacing (d) having X-ray wavelength λ and Bragg angle θ . The (111), (200), (220), (311) and (222) planes from XRD pattern satisfy with cubic phase of PbS. The lattice constant was estimated using the formula is given by

$$d = a / \sqrt{h^2 + k^2 + l^2} \quad (1)$$

where 'a' is lattice constant; h, k, and l are miller indices.

The interplanar spacing as well as the lattice constants go with the desired values and can be endorsed to cubic phase and confirm the creation of PbS nano particles.

The standard crystallite size (D) determined by using Scherrer formula,

$$D = 0.9\lambda / (\beta_{1/2} \cos \theta) \quad (2)$$

where x-ray having wavelength λ , $\beta_{1/2}$ is value of the full width at half maximum and θ is referred to Bragg angle. The normal crystalline size of PbS nanoparticles are measured approximately 5 nm

to 16 nm. Dislocation density and strain of grown nanoparticles are also determined. Lattice misfit confirms strain. The strain (μ) value have been calculated by the following formula

$$\mu = \beta_{1/2} \cot \theta / 4 \quad (3)$$

The calculated value of strain of different PbS nanoparticles are shown in Table 1, 2 and 3. From table, the strain data points out that the strain value decreases with temperature. The change may be attributed to the predominant crystallization process in nanoparticles. The calculated strain, dislocation density and particle size of prepared PbS nanoparticles are shown in Fig. 4.

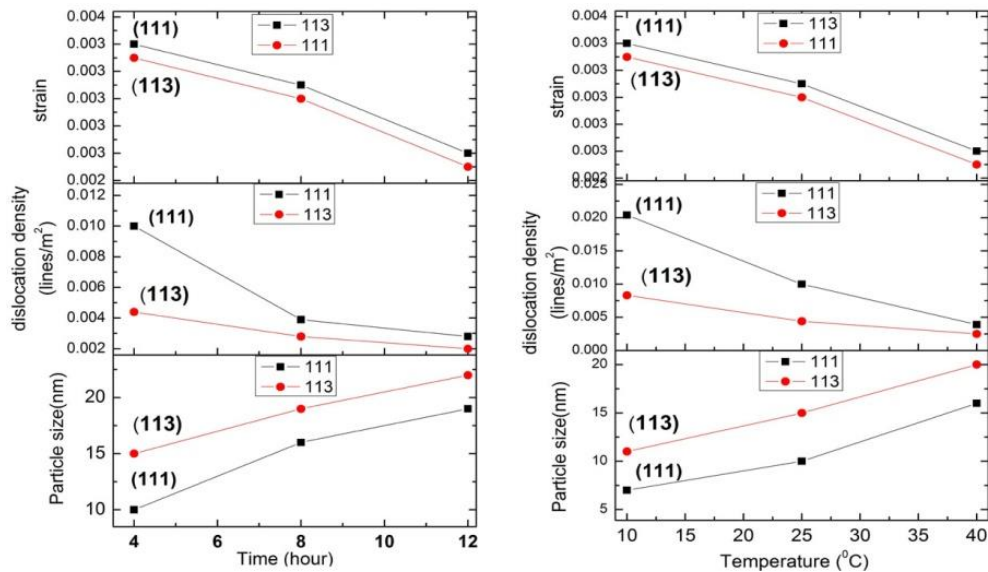


Fig. 4. The variation of particle size, dislocation density and strain of 1:1:1 and 1:1:3 PbS sample with growth time and temperature.

In a unit volume of the crystal we measure the length of dislocation lines as dislocation density. The presence of dislocation density strongly manipulates many of the properties of materials and is designated by dislocation density i.e. $\delta = (1 / D^2)$ (lines/m²). The lattice parameter, crystallite size, strain and dislocation density values were found for PbS (1:1:1) as well as PbS (1:1:3) sample grown for different time durations and temperatures. It is observed that with increase of particle size, dislocation density decreases. Thus in case of 1:1:5 sample and bulk material, the particle size becomes maximum and the defect parameters become minimum.

3.2. TEM Characterization

The TEM images of PbS samples with growth time are displayed in Fig. 5.

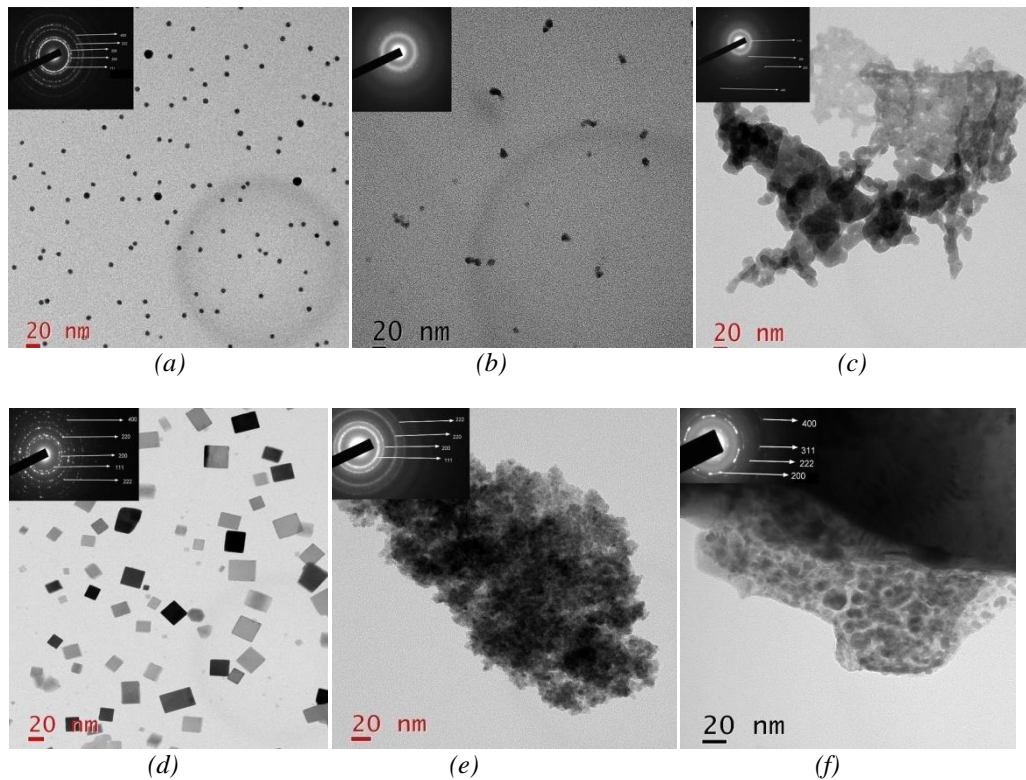


Fig.5. TEM images of PbS sample grown at different growth time 4h,8h and 12h with ratio 1:1:1 (a,b,c) and 1:1:3 (d,e,f) respectively.

For 1:1:1 ratio sample, the particle shape is spherical grown at room temperature. But with increase of growth time particle size increases and finally agglomerates. For ratio sample, the particle shape is cubic at room temperature. But with increase of growth time particle for 1:1:3 agglomerates in shorter duration compared to 1:1:1 sample.

For 1:1:1 ratio sample, the particle shape is spherical grown at room temperature. But with increase of growth time particle size increases and finally agglomerates. For ratio sample, the particle shape is cubic at room temperature. But with increase of growth time particle for 1:1:3 agglomerates in shorter duration compared to 1:1:1 sample.

Fig.6 reveals TEM images of PbS with growth temperature.

At low temperature the particles are well isolated. At room temperature the particle size is about 7 nm and the shape is spherical for 1:1:1sample. But particle size increases as temperature increases and finally agglomerates.

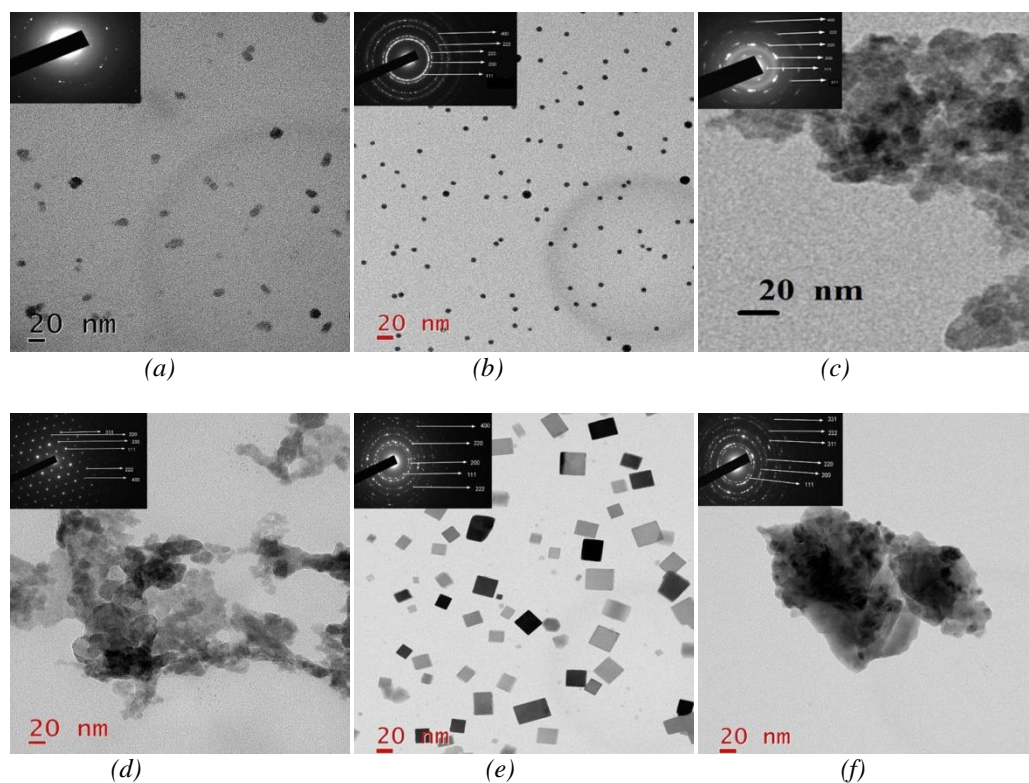


Fig.6. TEM images of PbS sample grown at different growth temperature 10°C, 25°C and 40°C with ratio 1:1:1 (a,b,c) and 1:1:3 (d,e,f) respectively.

The average size of the particle is 8 nm at ratio 1:1:3 and 10°C growth temperature. As we increase the temperature for 1:1:3 samples, the particle shape is cubic and size also increases at 25° C growth temperature. But with increase of temperature particles are mostly agglomerated. The particle size increases with increase of growth time in both ratios. This is possibly due to Ostwald ripening in which larger particles grow in exchange of smaller particles. As temperature increases the smaller particles become mobile and re crystallize to form larger particles. At higher reducing ratio 1:1:5 (Fig.7 (a)) the particles are totally agglomerated.

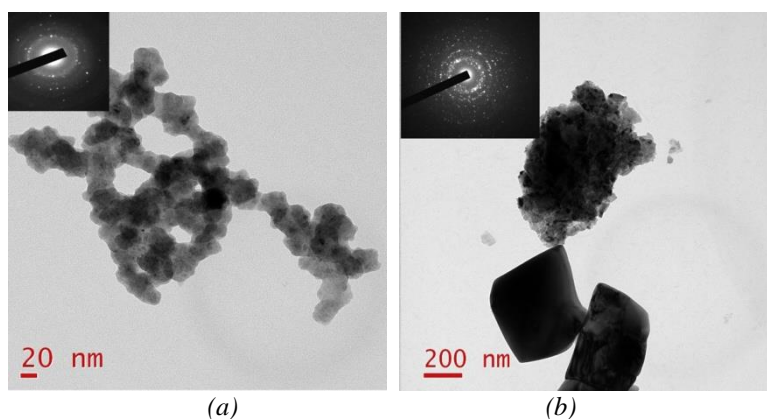


Fig. 7. TEM images of 1:1:5 PbS(a) and Bulk PbS(b).

This may be due to the excessive reduction of sulphur by the reducing agent. The Fig.7 (b) displays the TEM image of bulk PbS. The size increases drastically for bulk materials.

3.3. SEM Characterization

The SEM micrographs of prepared PbS nanoparticles are shown in Fig. 8, 9 and 10.

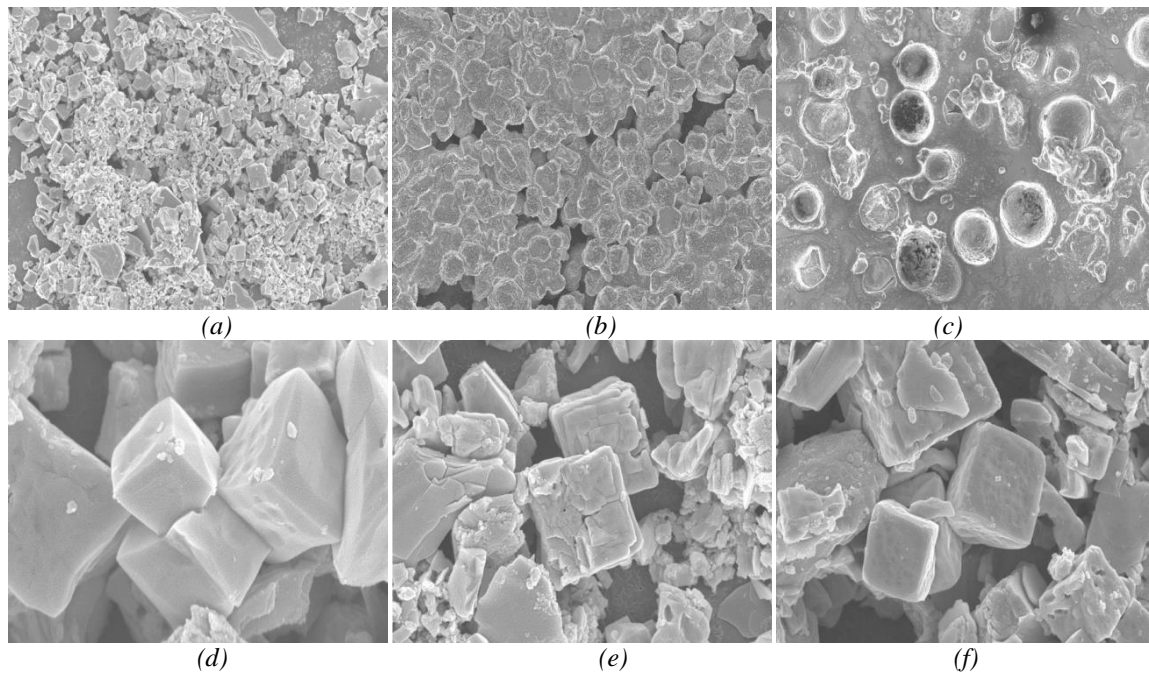


Fig. 8. SEM images of PbS sample grown at different growth time 4h, 8h and 12h with ratio 1:1:1 (a,b,c) and 1:1:3 (d,e,f).

SEM image (Fig. 8) indicates that the shape is spherical for 1:1:1 sample grown at different growth time. The shape is cubic for 1:1:3 samples.

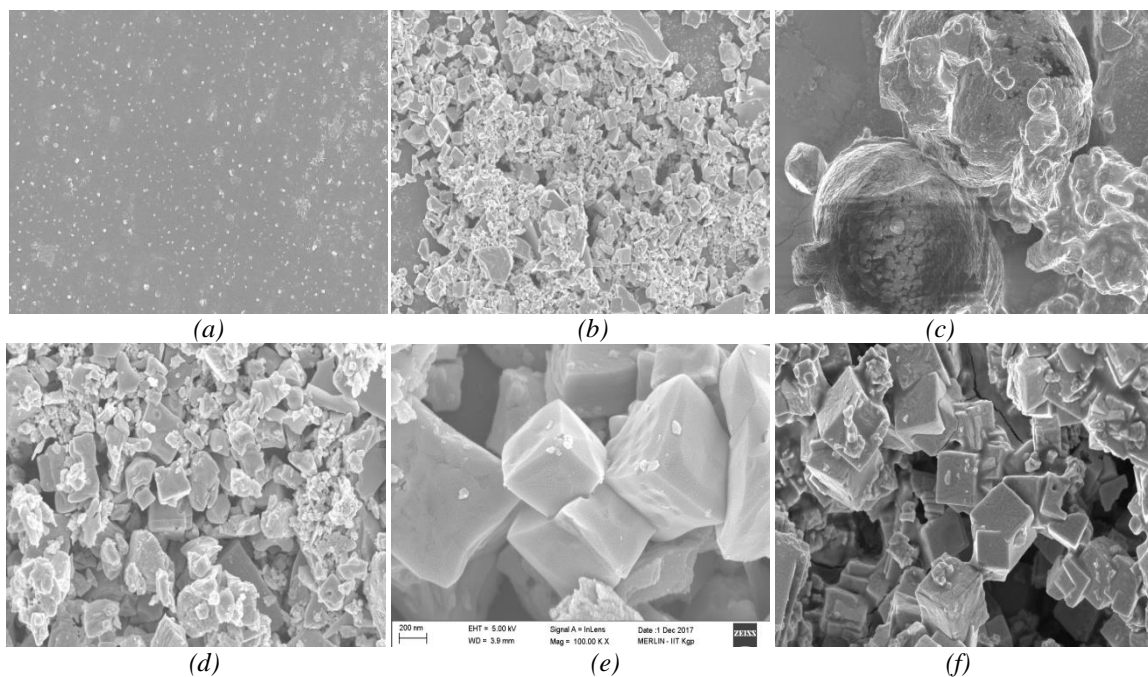


Fig. 9. SEM images of PbS sample grown at different growth temperature 10 °C, 25 °C and 40 °C with ratio 1:1:1 (a,b,c) and 1:1:3 (d,e,f).

The results are in agreement with the TEM result. SEM image (Fig. 9) indicates similarity with TEM also for samples grown at different temperatures.

Fibrous pattern is observed in SEM (Fig.10) for bulk PbS.

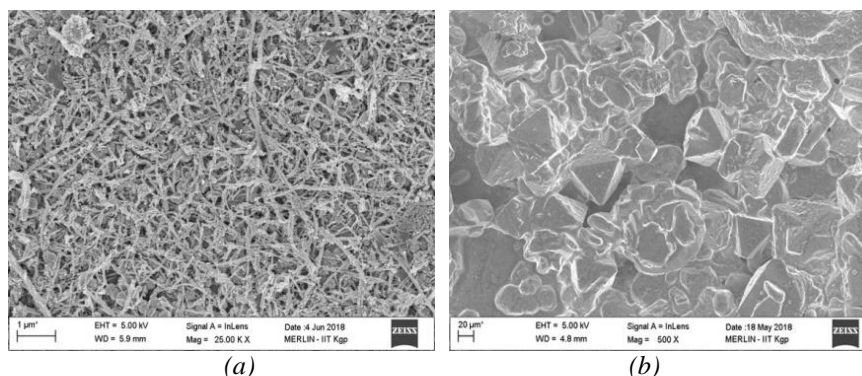


Fig. 10. SEM images of (a) Bulk PbS and (b) 1:1:5 PbS.

From EDX result it is clear that stoichiometry is well maintained for sample grown with capping agent EDA. At room temperature stoichiometry improves for both types of samples.

3.4. Optical measurement

The NIR absorption spectra of grown PbS samples are shown in Fig. 11 and 12.

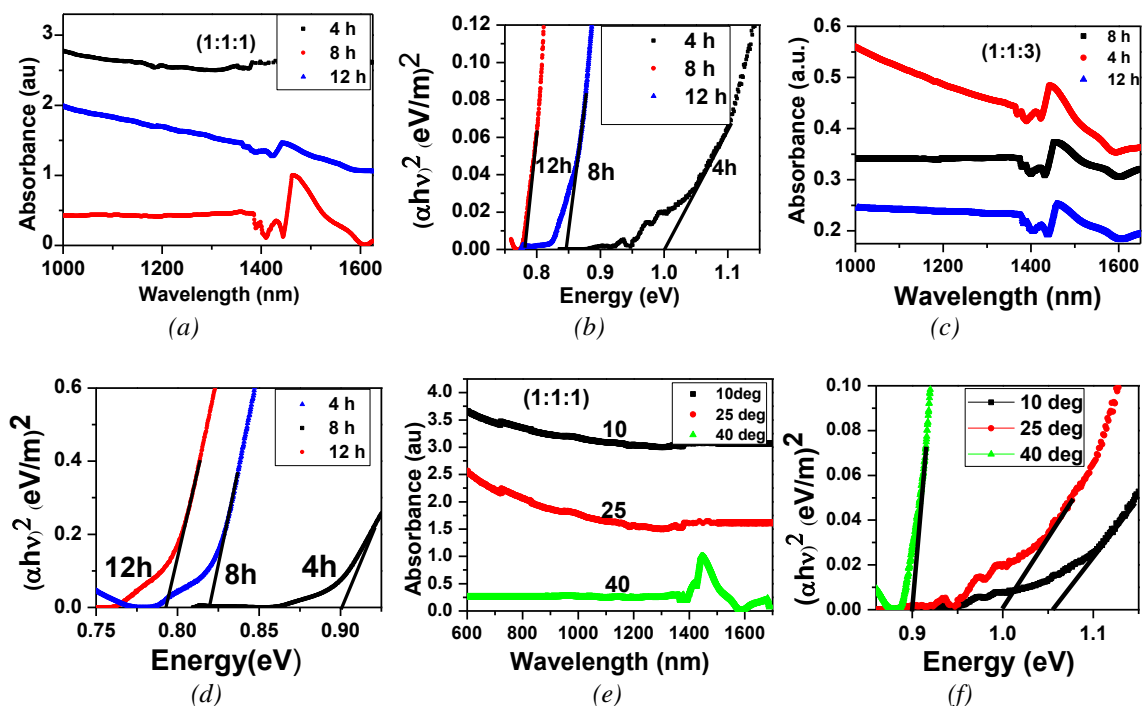


Fig. 11. NIR absorption spectrum and band gap determination of PbS sample at different growth time 4h, 8h, 12h with ratio 1:1:1(a,b), 1:1:3(c,d) and different temperature 10 °C, 25 °C, 40 °C with ratio 1:1:1(e,f)

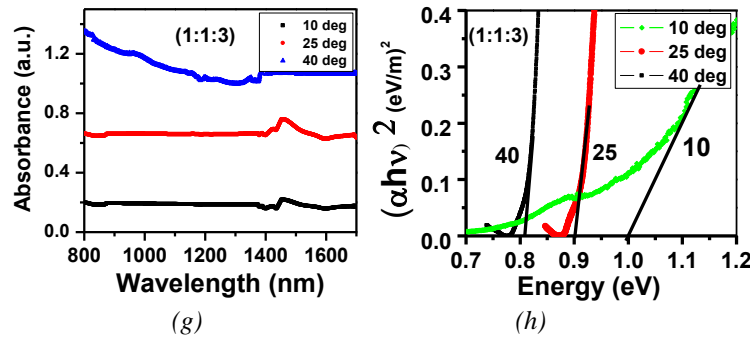


Fig. 11. NIR absorption spectrum and band gap determination of PbS sample at different growth time 4h, 8h, 12h with ratio 1:1:3(g,h).

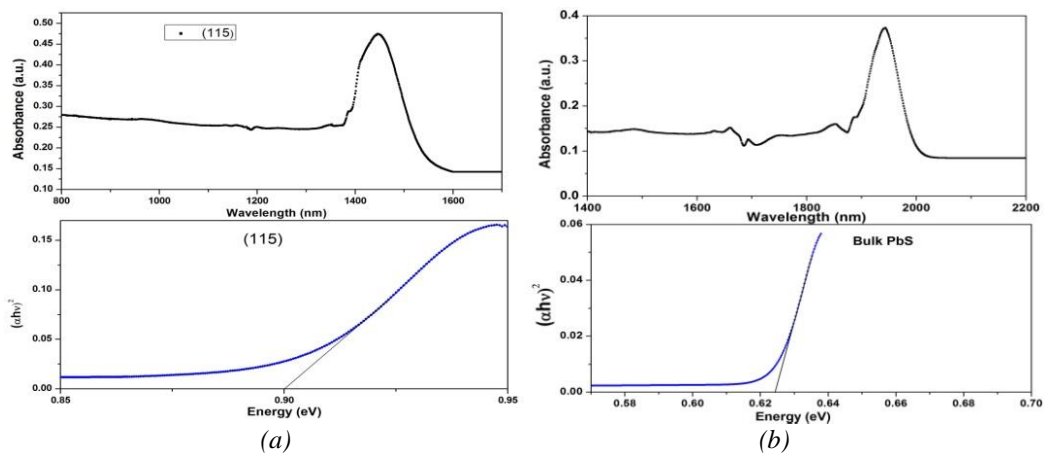


Fig. 12. NIR absorption spectrum of 1:1:5PbS sample(a) and of Bulk PbS sample(b).

The band gap of various nano samples are determined by Tauc relation $(\alpha h\nu)^2 = C(h\nu - E_g)$ Where α is absorption coefficient, h is Planck constant, ν is frequency, E_g is band gap and C is a constant. The band gap energy of the PbS nanoparticles decrease with increase of temperature as well as time duration of growth since the particle size increases in both conditions.

3.5. Fluorescence life time Measurement

Fig.13 and 14 show the fluorescence decay of grown PbS samples.

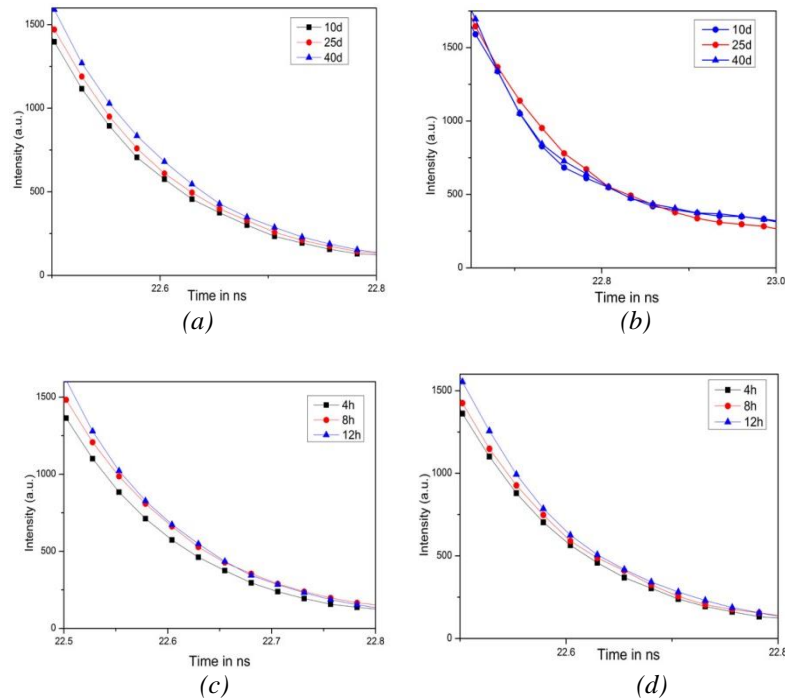


Fig.13. Fluorescence decay of PbS sample at different growth time 4h, 8h, 12h with ratio 1:1:1(a), 1:1:3(b) and different temperature 10 °C, 25°C, 40 °C with ratio 1:1:1(c), 1:1:3(d).

The electrons of specimen belong to energized state by absorbing photon and also come back in ground state by emitting photon. Fluorescence lifetime is defined by the average time which takes an electron to come back in ground state after absorbing photon. The decay of fluorescence in time is studied by fluorescence lifetime spectroscopy technique. The expression of exponential decay from an excited state to ground state is given by $I(t) = I_0 e^{-t/\tau}$ Where, I_0 is intensity of electron at initial time, $I(t)$ is Intensity of electron at time t , τ is Decay time. The lifetime is the time which is taken by the excited population to reach by a multiple of $1/e$ or 37 %.

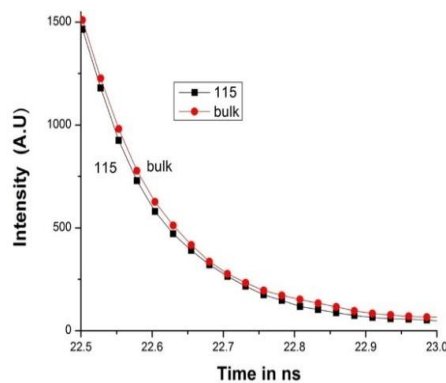


Fig. 14. The fluorescence decay of 1:1:5 PbS sample and bulk PbS with time.

Fluorescence lifetime measurement also does not depend on the concentration of the sample. The short pulse light source is used to excite the sample. When the pulse is generated, Time digitizer starts the counting with pulse generation and stops when emitted photon hits the detector. This lifetime is calculated by plotting the intensity of emitted photon with interval

between two signals. In logarithmic scale, we use single exponential fitting to calculate lifetime using the Origin Pro8.5 software. Fluorescence life time increases with increase of crystal size.

Table 1. Characteristics of PbS nanoparticles at different growth time.

PbS Sample	Time In hour	Size (nm) from TEM	Size (nm) from XRD	Strain(μ)= $B\cot\theta/4$	Dislocation density $\delta=(1/D^2)$ (lines/m ²)	Band gap (eV)	Atomic % (Pb & S) from EDX	Fluorescence lifetime in ps
1:1:1	4	7	10	0.0035	0.0100	1.0	46:54	27.3
	8	14	16	0.0030	0.0039	0.9	47:53	33.6
	12	17	19	0.0025	0.0028	0.79	44:56	42.8
1:1:3	4	12	15	0.0034	0.0044	0.94	52:48	28.3
	8	15	19	0.0031	0.0028	0.84	48:52	39.8
	12	18	22	0.0026	0.0020	0.78	46:54	49.2

Table 2. Characteristics of PbS nanoparticles at different growth temperature.

PbS Sample	Temperature In (^o C)	Size (nm) from TEM	Size (nm) from XRD	Strain(μ)= $B\cot\theta/4$	Dislocation density $\delta=(1/D^2)$ (lines/m ²)	Band gap(eV)	Atomic % (Pb & S) from EDX	Fluorescence lifetime in ps
1:1:1	10	5	7	0.0035	0.0204	1.1	43:57	17.2
	25	7	10	0.0033	0.0100	1.0	47:53	27.3
	40	13	16	0.0030	0.0039	0.9	57:43	33.6
1:1:3	10	8	11	0.0036	0.0083	1.0	58:42	24.4
	25	12	15	0.0034	0.0044	0.94	52:48	28.3
	40	16	20	0.0031	0.0025	0.80	54:46	37.7

Table 3. Characteristics of PbS nanoparticles grown at 25^oC of 1:1:5 ratio and bulk.

PbS Sample	Size (nm) from TEM	Size (nm) from XRD	Strain $\mu = B\cot\theta/4$	Dislocation density $\delta=(1/D^2)$ (lines/m ²)	Band gap(eV)	Atomic % of (Pb and S) from EDX	Fluorescence lifetime in ps
1:1:5	20	23	.0030	.0019	0.9	46:54	31.9
bulk	38	40	.0015	.0006	0.62	55:45	71.7

4. Conclusions

We found that the growth time and temperature controls the nanoparticles size. Consequently, the chemical reduction gives us good production quality as well as easy handling with high reproducibility. The increase of size of the crystal leads to decrease of strain and dislocation density. This is due to the decrease of surface area with increase of size. As a result the energy band gap changes from 0.62 eV to 1.1eV due to the size effect. The shape of the nanoparticles changes with variation of reducing agent ratio. The quantum confinement is good for spherical shaped sample at any temperature compared to cubic shaped sample. Thus we get the different morphological, optical and structural behavior of nanostructure with different growth time and temperature. Also TCSPC (Time-correlated single-photon counting) study indicates the

variation of fluorescence lifetime with shape as well as size of the crystal. Lifetime increases as the material changes from nanostructure to bulk structure.

Acknowledgements

Authors are grateful to UGC & DST for their constant support through SAP and FIST program to Department of Physics.

References

- [1] M. C. Weidman, M. E. Beck, R. S. Hoffman, F. Prins, W. A. Tisdale, *ACS nano* **8**, 6363 (2014).
- [2] S. A. McDonald, P. W. Cyr, L. Levina, E. H. Sargent, *Appl. Phys. Lett.* **85**, 11 (2004).
- [3] M. M. Abbas, A. A. M. Shehabb, A. K. A. Samuraec, N. A. Hassan, *Energy Procedia* **6**, 241 (2011).
- [4] G. Nabyouni, P. Boroojerdian, K. Hedayati, D. Ghanbari, *High Temp. Mater. Proc.* **31**, 723 (2012).
- [5] J. R. Caram, S. N. Bertram, H. Utzat, W. R. Hess, J. A. Carr, T. S. Bischof, A. P. Beyler, M. W. B. Wilson, M. G. Bawendi, *Nano Lett.* **16**, 6070 (2016).
- [6] S. B. Pawara, J. S. Shaikhb, R. S. Devanc, Y. R. Mac, D. Haranathd, P. N. Bhosalea, P. S. Patil, *Applied Surface Science* **258**, 1869 (2011).
- [7] K. K. Nanda, F. E. Kruis, H. Fissan, *J. Appl. Phys.* **95**, 9 (2004).
- [8] S. J. O. Hardman, D. M. Graham, S. K. Stubbs, B. F. Spencer, E. A. Seddon, H. Fung, S. Gardonio, F. Sirotti, M. G. Silly, J. Akhtar, P. O'Brien, D. J. Binksa, W. R. Flavella, *Phys. Chem. Chem. Phys.* **13**, 20275 (2011).
- [9] D. Himadri, D. Pranayee, S. Kandarpa Kumar, *Journal of Nanoscience and Technology* **4**(5), 500 (2018).
- [10] L. S. Chongad, A. Sharma, M. Banerjee, *A. Jain Journal of Physics Conference Series* **755**, 012032 (2016).
- [11] R. S. Mane, C. D. Lokhande *Materials Chemistry and Physics* **65**, 1 (2000).
- [12] Z. Huang, G. Zhai, Z. Zhang, C. Zhang, Y. Xia, L. Lian, X. Fu, D. Zhang, J. Zhang, *Cryst. Eng. Comm.* **19**, 946 (2017).
- [13] G. Nabyouni, P. Boroojerdian, K. Hedayati, D. Ghanbari, *High Temp. Mater. Proc.* **31**, 723 (2012).
- [14] M. M. Abbas, A. A. M. Shehabb, A. K. A. Samuraec, N. A. Hassan *Energy Procedia* **6**, 241 (2011).
- [15] A. Pourahmad, *Arabian Journal of Chemistry* **7**, 788 (2014).
- [16] L. Chen, H. Liu, L. Liu, Y. Zheng, H. Tang, Z. Liu *Crystals* **8**, 397 (2018).
- [17] P. Dey, J. Paul, J. Bylsmaa, D. Karaiskaj, J. M. Luther, M. C. Beard, A. H. Romero, *Solid State Communications* **165**, 49 (2013).
- [18] J. R. Caram, S. N. Bertram, H. Utzat, W. R. Hess, J. A. Carr, T. S. Bischof, A. P. Beyler, M. W. B. Wilson, M. G. Bawendi, *Nano Lett.* **16**, 6070 (2016).
- [19] H. Zhao, H. Liang, F. Vidal, F. Rosei, A. Vomiero, D. Ma *J. Phys. Chem. C* **118**, 20585 (2014).
- [20] R. P. Merino, R. G. Pérez, P. T. García, L. C. Lima, O. P. Moreno, M. E. A. García, A. M. Rodriguez, E. R. Rosas, *Journal of Nanomaterials* **15**, 3431942 (2018).
- [21] D. M. Balazs, D. N. Dirin, H. H. Fang, L. Protesescu, G. H. ten Brink, B. J. Kooi, M. V. Kovalenko, M. A. Loi, *Acs Nano* **9**, 11951 (2015).
- [22] M. L. Kessler, H. E. Starr, R. R. Knauf, K. J. Rountree, J. L. Dempsey, *Physical Chemistry Chemical Physics* **36**, 23649 (2018).
- [23] A. Bhardwaj, A. Hreibi, C. Liu, J. Heo, J. M. Blondy, F. Gérôme, *Optics Express* **21**, 21 (2013).

- [24] H. Karami, M. Ghasemi, S. Matini, *Int. J. Electrochem. Sci.* **8**, 11661 (2013).
- [25] A. A. Ibrahim, *Defect and Diffusion Forum* **294**, 85 (2009).
- [26] R. Jin, G. Chen, J. Pei, *J. Phys. Chem. C* **116**, 16207 (2012).